

Cite this: *Chem. Commun.*, 2012, **48**, 2015–2017

www.rsc.org/chemcomm

## COMMUNICATION

## Anomalous thermal transition and crystallization of ionic liquids confined in graphene multilayers†

Jinkyu Im,<sup>a</sup> Sung Dae Cho,<sup>b</sup> Min Hye Kim,<sup>b</sup> Young Mee Jung,<sup>c</sup> Hoon Sik Kim<sup>\*a</sup> and Ho Seok Park<sup>\*b</sup>

Received 13th October 2011, Accepted 12th December 2011

DOI: 10.1039/c2cc16367e

**Anomalous thermal transition and crystallization behaviors of three room temperature ionic liquids (RTILs) in graphene multilayers (GMLs), in a different manner to bulk RTILs, occurred due to the molecular orientation of the confined system triggered by the complex  $\pi$ - $\pi$  stacking and hydrogen bonding interactions.**

There is considerable interest in the confinement of molecular and organic solvents, biomolecules, polymers, and ionic liquids in a nanometric space.<sup>1</sup> The nanoconfinement effect on the unique thermal properties and anomalous phase behaviours of guest materials has been investigated for both fundamental understanding of nanoscience and transport, tribology, adhesion, and fluidic applications.<sup>2</sup>

Room-temperature ionic liquids (RTILs), which are composed of large organic cations and weakly coordinating anions, are regarded as environmentally benign solvents offering a wide range of applications as solvents, in catalysis, electrochemistry, and separation.<sup>3</sup> The thermal properties and phase behaviours of RTILs can be tailored by the complex interplay of interactions.<sup>4</sup> In particular, RTILs under nanometric spatial constraints revealed intriguing and unexpected thermal and phase behaviours as confined fluids.<sup>5</sup> For instance, RTILs confined in carbon nanotubes formed polymorphous crystals with a melting point of  $> 200$  °C.<sup>6</sup> Moreover, we demonstrated high ionic conductivity and phase transition of RTILs confined in aluminium hydroxide nanostructures.<sup>7</sup> Motivated by these significant studies, we report the thermal transition and crystallization of RTILs within the layers of two-dimensional (2D) graphenes.

Recently, graphenes have advanced the field of 2D nanomaterials because of their remarkable electronic, optical, and thermal properties, chemical and mechanical stability, and large surface area.<sup>8</sup> For practical applications in a bulk system,

graphene-based objects were assembled from the multilayers of exfoliated sheets.<sup>9</sup> The multilayered graphenes and graphene oxides are weakly stacked along the *c*-axis perpendicular to the sheets, in a different manner from graphite, which is strictly defined by  $\pi$ - $\pi$  interactions.<sup>10</sup> For the confined system within graphene multilayers (GMLs), water molecules show anisotropic ionic transport and colossal pressure.<sup>11</sup> Despite intensive efforts, the thermal and phase transitions of RTILs confined in GMLs remain unexplored.

Herein, we report the dramatic melting point enhancement and crystallization of RTILs confined in GMLs. The thermal and phase behaviours of confined RTILs, which were extensively analyzed by spectroscopic methods, were strongly influenced by the anion type.

In this research, 1-butyl-3-methylimidazolium tetrafluoroborate ([bmim][BF<sub>4</sub>]), 1-butyl-3-methylimidazolium hexafluorophosphate ([bmim][PF<sub>6</sub>]), and 1-butyl-3-methylimidazolium bis(trifluoromethanesulfonyl)amide ([bmim][Tf<sub>2</sub>N]) RTILs were used as confined fluids. The described RTILs are composed of identical imidazolium cations with different anions. GMLs were synthesized with the previously described solution chemistry and RTILs were confined in GMLs through mechanical grinding (see ESI†).<sup>12</sup> The confined RTILs inside the layers of GMLs were defined as [bmim][BF<sub>4</sub>]@GML, [bmim][PF<sub>6</sub>]@GML, and [bmim][Tf<sub>2</sub>N]@GML.

Fig. 1 shows differential scanning calorimetry (DSC) curves of three pristine RTILs, [bmim][BF<sub>4</sub>]@GML, [bmim][PF<sub>6</sub>]@GML, and [bmim][Tf<sub>2</sub>N]@GML, measured in the range of  $-80$  °C to  $150$  °C. The thermal properties of RTILs@GMLs were analyzed at the second heating cycle. The bulk [bmim][BF<sub>4</sub>] revealed a glass transition temperature ( $T_g$ ) of  $-71.4$  °C, while the  $T_g$  of [bmim][BF<sub>4</sub>]@GML was shifted to higher temperatures of  $-56.1$  °C and  $-42.5$  °C. Therefore, after confinement in the GMLs, the mobility of [bmim][BF<sub>4</sub>] was reduced due to the different chemical environment and spatial restriction. Moreover, the additional on-set temperature of the broad endothermic peak in the [bmim][BF<sub>4</sub>]@GML appeared at around  $-6.8$  °C. Neither the  $T_g$  nor the melting temperature ( $T_m$ ) of the bulk [bmim][PF<sub>6</sub>] was observed in this measurement range. In contrast, [bmim][PF<sub>6</sub>]@GML generated two emerging endothermic peaks near  $-15.5$  °C and  $3.3$  °C due to the molecular orientation of the RTILs. In particular, [bmim][PF<sub>6</sub>]@GML exhibited a much sharper endothermic peak compared to [bmim][BF<sub>4</sub>]@GML

<sup>a</sup> Department of Chemistry and Research Institute of Basic Sciences, Kyung Hee University, 1 Hoegidong, Dongdamoongu, Seoul, Republic of Korea

<sup>b</sup> Department of Chemical Engineering, College of Engineering, Kyung Hee University, 1 Seochon-dong, Giheung-gu, Youngin-si, Gyeonggi-do 446-701, Republic of Korea. E-mail: phs0727@khu.ac.kr

<sup>c</sup> Department of Chemistry and Institute for Molecular Science and Fusion Technology, Kangwon National University, Chuncheon 200-701, Republic of Korea

† Electronic supplementary information (ESI) available: Experimental section and additional characterization data. See DOI: 10.1039/c2cc16367e

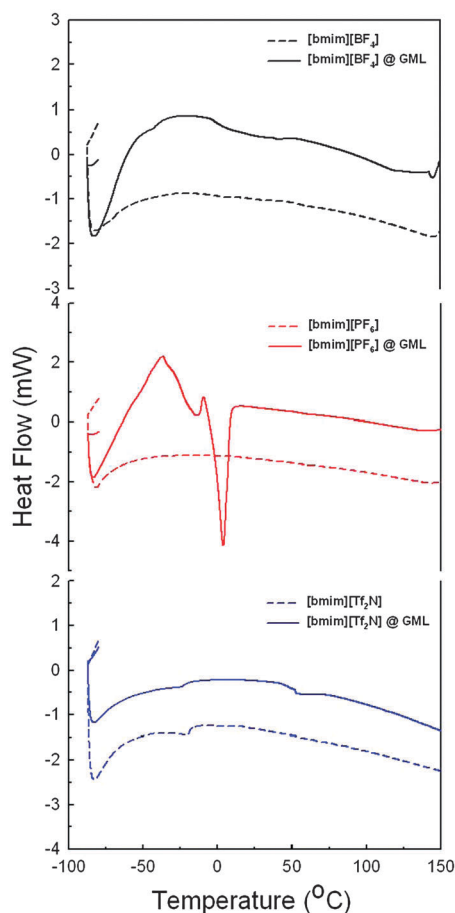


**Fig. 1** DSC curves of [bmim][BF<sub>4</sub>] and [bmim][BF<sub>4</sub>]@GML (top), [bmim][PF<sub>6</sub>] and [bmim][PF<sub>6</sub>]@GML (middle), and [bmim][Tf<sub>2</sub>N] and [bmim][Tf<sub>2</sub>N]@GML (bottom).

because of more favourable crystallization. In contrast, [bmim][Tf<sub>2</sub>N]@GML showed different phase behaviours from the afore-mentioned two RTILs@GMLs. The endothermic peak of bulk [bmim][Tf<sub>2</sub>N] at around  $-22.2^{\circ}\text{C}$  was weaker and shifted, while a new endothermic peak appeared near  $52.8^{\circ}\text{C}$  with the confinement of RTILs within the GML layers. These findings illustrate different crystallization and thermal transition behaviours of confined RTILs from those of bulk RTILs.

X-Ray diffraction (XRD) spectroscopy was used as the emergence of endothermic peaks was closely related to the crystallization of RTILs accommodated in the nanospace of GMLs. XRD patterns of the three RTILs@GMLs were compared to those of the three bulk RTILs (Fig. 2). XRD peaks of GMLs were not observed due to the small volume fraction relative to RTILs. The characteristic peaks of the three RTILs@GMLs at around  $19^{\circ}$  corresponded to imidazolium ring ordering in an analogous manner to the aggregation of bulk RTILs. Moreover, [bmim][BF<sub>4</sub>]@GML and [bmim][PF<sub>6</sub>]@GML revealed the emerging peaks at around  $54^{\circ}$  and  $57^{\circ}$  due to the hydrogen bonding between the acidic hydrogen of the imidazolium ring and the anion. Although the locations of additional peaks of the two RTILs@GMLs were nearly consistent, the intensity of [bmim][PF<sub>6</sub>]@GML was much greater than that of [bmim][BF<sub>4</sub>]@GML. This finding could be closely related to the strong endothermic peak of

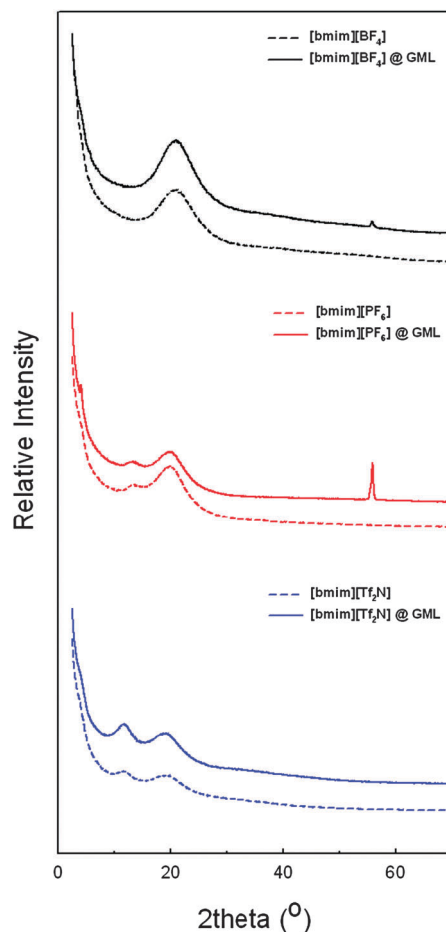


**Fig. 2** XRD patterns of [bmim][BF<sub>4</sub>] and [bmim][BF<sub>4</sub>]@GML (top), [bmim][PF<sub>6</sub>] and [bmim][PF<sub>6</sub>]@GML (middle), and [bmim][Tf<sub>2</sub>N] and [bmim][Tf<sub>2</sub>N]@GML (bottom).

[bmim][PF<sub>6</sub>]@GML due to the favourable molecular orientation. In contrast, [bmim][Tf<sub>2</sub>N]@GML produced the same XRD pattern as that of bulk RTIL. However, two peaks of [bmim][Tf<sub>2</sub>N] at around  $12^{\circ}$  and  $19^{\circ}$  were strengthened after incorporation into the layers of GML. In particular, the relative intensities of the two peaks were reversed for the [bmim][Tf<sub>2</sub>N]@GML and the peak at  $12^{\circ}$  was strengthened due to a more favourable orientation of RTIL than that of bulk RTIL. The transformation of [bmim][Tf<sub>2</sub>N] RTILs within the GML layers from a broad aggregation peak to a sharp crystalline peak corroborated the appearance of an endothermic peak at around  $52.8^{\circ}\text{C}$ , corresponding to the different physicochemical circumstances. Consequently, the anomalous phase behaviours of [bmim][BF<sub>4</sub>], [bmim][PF<sub>6</sub>], and [bmim][Tf<sub>2</sub>N] within the GMLs were strongly influenced by the anion type, thereby generating the respective thermal transition behaviours that were not observed in a bulk phase.

The molecular orientation and rearrangement of RTILs triggered in the 2D nanospace invokes the unexpected phase transition behaviours attributed to crystallization that were not detected in the bulk system. This unusual thermal transition and crystallization in the nanometric system are strongly influenced by the geometric constraints and the strong interactions between the solid and fluid, as explained by Gibbs–Thomson equation.<sup>13</sup>

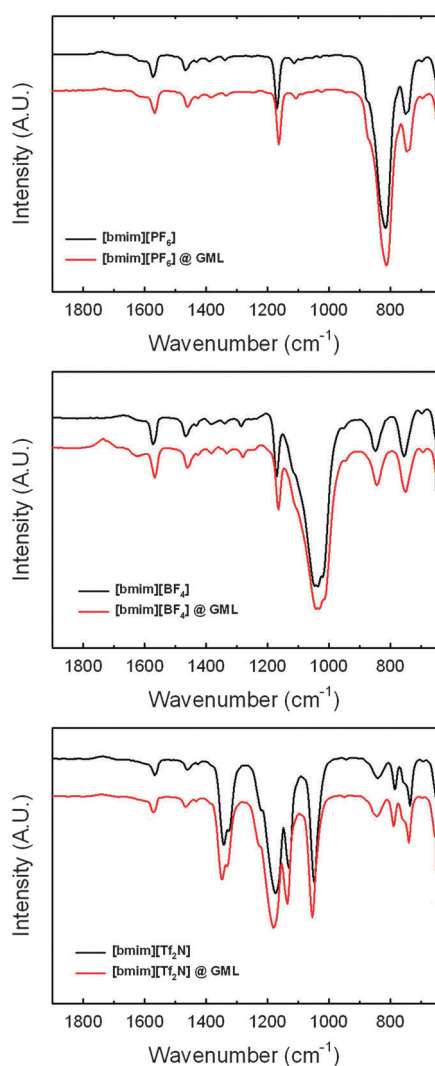


**Fig. 3** FT-IR spectra of [bmim][BF<sub>4</sub>] and [bmim][BF<sub>4</sub>]@GML (top), [bmim][PF<sub>6</sub>] and [bmim][PF<sub>6</sub>]@GML (middle), and [bmim][Tf<sub>2</sub>N] and [bmim][Tf<sub>2</sub>N]@GML (bottom).

The structure of an RTIL is determined by an energetic balance between  $\pi$ - $\pi$  stacking and hydrogen bonding interactions.<sup>3</sup> Thus, it is postulated that the three RTILs@GMLs showed different thermal behaviours with respect to the specific interactions because of the identical geometric constraints of the GMLs. FT-IR spectroscopy was used to verify the interactions between RTILs and GMLs, as shown in Fig. 3. The characteristic bands of the imidazolium ring in RTILs appeared at approximately 1570 cm<sup>-1</sup>, 1460 cm<sup>-1</sup>, 1170 cm<sup>-1</sup>, and 850 cm<sup>-1</sup> (see ESI†). These bands shifted to lower wavenumbers due to the  $\pi$ - $\pi$  stacking interactions between the imidazolium rings of RTILs and the conjugation of GMLs. Two peaks above 3000 cm<sup>-1</sup> in the IR spectra of [bmim][BF<sub>4</sub>], [bmim][PF<sub>6</sub>], and [bmim][Tf<sub>2</sub>N] were considered to result from the changes in the hydrogen bonding networks between the anions and the C(4, 5)-hydrogens of the imidazolium ring. In the confined system, these bands were also red-shifted because of the complicated interplay of hydrogen bonding interactions. This result was supported by UV and Raman spectra of the three RTILs@GMLs (see ESI†).<sup>14</sup>

It means that the respective  $\pi$ - $\pi$  stacking and hydrogen bonding interactions of RTILs@GMLs in accordance with the anion type resulted in different thermal transition behaviors.

From these results, it is obvious that the thermal transition and crystallization behaviors of bulk RTILs are dramatically changed when confined in graphenes. Moreover, the influence of anions on the thermal transition and crystallization of the confined system indicated that the molecular orientations of RTILs confined in the GML layers were dependent on the  $\pi$ - $\pi$  stacking and hydrogen bonding interactions.

We acknowledge the financial support by both the National Research Foundation (NRF) funded by the Korean Government (MEST) (20090063004) and NRF-2010-C1AAA001-0029018 and Basic Science Research Program through the National Research Foundation of Korea (NRF) funded by the Ministry of Education, Science and Technology (2011-0007677).

## Notes and references

- 1 K. Koga, G. T. Gao, H. Tanaka and X. C. Zeng, *Nature*, 2001, **412**, 802; T. S. Kim and R. H. Dauskardt, *Nano Lett.*, 2010, **10**, 1955; S. Zhu, Y. Liu, M. H. Rafailovich, J. Sokolov, D. Gersappe, D. A. Winesett and H. Ade, *Nature*, 1999, **400**, 49.
- 2 W. T. S. Huck, *Chem. Commun.*, 2005, 4143; M. Alcoutlabi and G. B. McKenna, *J. Phys.: Condens. Matter*, 2005, **17**, R461.
- 3 T. Welton, *Chem. Rev.*, 1999, **99**, 2071; J. Dupont, R. F. de Souza and P. A. Z. Suarez, *Chem. Rev.*, 2002, **102**, 3667; L. A. Blanchard, D. Hancu, E. J. Beckman and J. F. Brennecke, *Nature*, 1999, **399**, 28.
- 4 T. A. Bleasdale, G. J. T. Tiddy and E. Wyn-Jones, *J. Phys. Chem.*, 1991, **95**, 5385; F. Neve, O. Francescangeli and A. Crispini, *Inorg. Chim. Acta*, 2002, **338**, 51; J. L. Anthony, E. J. Maginn and J. F. Brennecke, *J. Phys. Chem. B*, 2001, **105**, 10942.
- 5 M. Kanakubo, Y. Hiejima, K. Minami, T. Aizawa and H. Nanjo, *Chem. Commun.*, 2006, 1828; M. Sha, G. Wu, Y. Liu, Z. Tang and H. Fang, *J. Phys. Chem. C*, 2009, **113**, 4618.
- 6 S. Chen, K. Kobayashi, Y. Miyata, N. Imazu, T. Saito, R. Kitaura and H. Shinohara, *J. Am. Chem. Soc.*, 2009, **131**, 14850; S. Chen, G. Wu, M. Sha and S. Huang, *J. Am. Chem. Soc.*, 2007, **129**, 2416.
- 7 H. S. Park, Y. S. Choi, Y. M. Jung and W. H. Hong, *J. Am. Chem. Soc.*, 2008, **130**, 845; H. S. Park, Y. S. Choi, Y. J. Kim, W. H. Hong and H. Song, *Adv. Funct. Mater.*, 2007, **17**, 2411.
- 8 X. Li, X. Wang, L. Zhang, S. Lee and H. Dai, *Science*, 2008, **319**, 1229; P. Schedin, A. K. Geim, S. V. Morozov, E. W. Hill, P. Blake, M. I. Katsnelson and K. S. Novoselov, *Nat. Mater.*, 2007, **6**, 652; N. Mohanty and V. Berry, *Nano Lett.*, 2008, **8**, 4469; M. D. Stoller, S. Park, Y. Zhu, J. An and R. S. Ruoff, *Nano Lett.*, 2008, **8**, 3498.
- 9 B. G. Choi, J. Hong, W. H. Hong, P. T. Hammond and H. S. Park, *ACS Nano*, 2011, **5**, 7205; B. G. Choi, J. Hong, Y. C. Park, D. H. Jung, W. H. Hong, P. T. Hammond and H. S. Park, *ACS Nano*, 2011, **5**, 5167; Z. Chen, W. Ren, L. Gao, B. Liu, S. Pei and H. M. Cheng, *Nat. Mater.*, 2011, **10**, 424; Y. Xu, K. Sheng, C. Li and G. Shi, *ACS Nano*, 2010, **4**, 4324.
- 10 S. Park, K. S. Lee, G. Bozoklu, W. Cai, S. B. T. Nguyen and R. S. Ruoff, *ACS Nano*, 2008, **2**, 572; M. Acik, C. Mattevi, C. Gong, G. Lee, K. Cho, M. Chhowalla and Y. J. Chabal, *ACS Nano*, 2010, **4**, 5861.
- 11 W. Gao, N. Singh, L. Song, Z. Liu, A. L. M. Reddy, L. Ci, R. Vajtai, Q. Zhang, B. Wei and P. M. Ajayan, *Nat. Nanotechnol.*, 2011, **6**, 496; A. V. Talyzin, V. L. Solozhenko, O. O. Kurakevych, T. Szabó, I. Dékány, A. Kurnosov and V. Dmitriev, *Angew. Chem., Int. Ed.*, 2008, **47**, 8268.
- 12 B. G. Choi, H. S. Park, T. J. Park, M. H. Yang, J. S. Kim, S. Y. Jang, N. S. Heo, S. Y. Lee, J. Kong and W. H. Hong, *ACS Nano*, 2010, **4**, 2910; P. Du, S. Liu, P. Wu and C. Cai, *Electrochim. Acta*, 2007, **52**, 6534.
- 13 H. K. Christenson, *J. Phys.: Condens. Matter*, 2001, **13**, R95.
- 14 B. G. Choi, W. H. Hong, Y. M. Jung and H. S. Park, *Chem. Commun.*, 2011, **47**, 10293.